Measurements of the branching fractions of $\psi(3686) \to \bar{\Sigma}^0\Lambda + \mathrm{c.c.}$ and $\chi_{cJ(J=0,1,2)} \to \Lambda\bar{\Lambda}$

M. Ablikim,[1] M. N. Achasov,[10,c] P. Adlarson,[67] S. Ahmed,[15] M. Albrecht,[4] R. Aliberti,[28] A. Amoroso,[66a,66c] M. R. An,[32] Q. An,[63,49] X. H. Bai,[57] Y. Bai,[48] O. Bakina,[29] R. Baldini Ferroli,[23a] I. Balossino,[24a] Y. Ban,[38,k] K. Begzsuren,[26] N. Berger,[28] M. Bertani,[23a] D. Bettoni,[24a] F. Bianchi,[66a,66c] J. Bloms,[60] A. Bortone,[66a,66c] I. Boyko,[29] R. A. Briere,[5] H. Cai,[68] X. Cai,[1,49] A. Calcaterra,[23a] G. F. Cao,[1,54] N. Cao,[1,54] S. A. Cetin,[53a] J. F. Chang,[1,49] W. L. Chang,[1,54] G. Chelkov,[29,b] D. Y. Chen,[6] G. Chen,[1] H. S. Chen,[1,54] M. L. Chen,[1,49] S. J. Chen,[35] X. R. Chen,[25] Y. B. Chen,[1,49] Z. J. Chen,[20,l] W. S. Cheng,[66c] G. Cibinetto,[24a] F. Cossio,[66c] X. F. Cui,[36] H. L. Dai,[1,49] X. C. Dai,[1,54] A. Dbeyssi,[15] R. E. de Boer,[4] D. Dedovich,[29] Z. Y. Deng,[1] A. Denig,[28] I. Denysenko,[29] M. Destefanis,[66a,66c] F. De Mori,[66a,66c] Y. Ding,[33] C. Dong,[36] J. Dong,[1,49] L. Y. Dong,[1,54] M. Y. Dong,[1,49,54] X. Dong,[68] S. X. Du,[71] Y. L. Fan,[68] J. Fang,[1,49] S. S. Fang,[1,54] Y. Fang,[1] R. Farinelli,[24a] L. Fava,[66b,66c] F. Feldbauer,[4] G. Felici,[23a] C. Q. Feng,[63,49] J. H. Feng,[50] M. Fritsch,[4] C. D. Fu,[1] Y. Gao,[63,49] Y. Gao,[38,k] Y. Gao,[64] Y. G. Gao,[6] I. Garzia,[24a,24b] P. T. Ge,[68] C. Geng,[50] E. M. Gersabeck,[58] A. Gilman,[61] K. Goetzen,[11] L. Gong,[33] W. X. Gong,[1,49] W. Gradl,[28] M. Greco,[66a,66c] L. M. Gu,[35] M. H. Gu,[1,49] S. Gu,[2] Y. T. Gu,[13] C. Y. Guan,[1,54] A. Q. Guo,[22] L. B. Guo,[34] R. P. Guo,[40] Y. P. Guo,[9,h] A. Guskov,[29] T. T. Han,[41] W. Y. Han,[32] X. Q. Hao,[16] F. A. Harris,[56] N. Hüsken,[22,28] K. L. He,[1,54] F. H. Heinsius,[4] C. H. Heinz,[28] T. Held,[4] Y. K. Heng,[1,49,54] C. Herold,[51] M. Himmelreich,[11,f] T. Holtmann,[4] Y. R. Hou,[54] Z. L. Hou,[1] H. M. Hu,[1,54] J. F. Hu,[47,m] T. Hu,[1,49,54] Y. Hu,[1] G. S. Huang,[63,49] L. Q. Huang,[64] X. T. Huang,[41] Y. P. Huang,[1] Z. Huang,[38,k] T. Hussain,[65] W. Ikegami Andersson,[67] W. Imoehl,[22] M. Irshad,[63,49] S. Jaeger,[4] S. Janchiv,[26,j] Q. Ji,[1] Q. P. Ji,[16] X. B. Ji,[1,54] X. L. Ji,[1,49] Y. Y. Ji,[41] H. B. Jiang,[41] X. S. Jiang,[1,49,54] J. B. Jiao,[41] Z. Jiao,[18] S. Jin,[35] Y. Jin,[57] T. Johansson,[67] N. Kalantar-Nayestanaki,[55] X. S. Kang,[33] R. Kappert,[55] M. Kavatsyuk,[55] B. C. Ke,[43,1] I. K. Keshk,[4] A. Khoukaz,[60] P. Kiese,[28] R. Kiuchi,[1] R. Kliemt,[11] L. Koch,[30] O. B. Kolcu,[53a,e] B. Kopf,[4] M. Kuemmel,[4] M. Kuessner,[4] A. Kupsc,[67] M. G. Kurth,[1,54] W. Kühn,[30] J. J. Lane,[58] J. S. Lange,[30] P. Larin,[15] A. Lavania,[21] L. Lavezzi,[66a,66c] Z. H. Lei,[63,49] H. Leithoff,[28] M. Lellmann,[28] T. Lenz,[28] C. Li,[39] C. H. Li,[32] Cheng Li,[63,49] D. M. Li,[71] F. Li,[1,49] G. Li,[1] H. Li,[63,49] H. Li,[43] H. B. Li,[1,54] H. J. Li,[16] J. L. Li,[41] J. Q. Li,[4] J. S. Li,[50] Ke Li,[1] L. K. Li,[1] Lei Li,[3] P. R. Li,[31] S. Y. Li,[52] W. D. Li,[1,54] W. G. Li,[1] X. H. Li,[63,49] X. L. Li,[41] Xiaoyu Li,[1,54] Z. Y. Li,[50] H. Liang,[1,54] H. Liang,[63,49] H. Liang,[27] Y. F. Liang,[45] Y. T. Liang,[25] G. R. Liao,[12] L. Z. Liao,[1,54] J. Libby,[21] C. X. Lin,[50] B. J. Liu,[1] C. X. Liu,[1] D. Liu,[63,49] F. H. Liu,[44] Fang Liu,[1] Feng Liu,[6] H. B. Liu,[13] H. M. Liu,[1,54] Huanhuan Liu,[1] Huihui Liu,[17] J. B. Liu,[63,49] J. L. Liu,[64] J. Y. Liu,[1,54] K. Liu,[1] K. Y. Liu,[33] Ke Liu,[6] L. Liu,[63,49] M. H. Liu,[9,h] P. L. Liu,[1] Q. Liu,[54] Q. Liu,[68] S. B. Liu,[63,49] Shuai Liu,[46] T. Liu,[1,54] W. M. Liu,[63,49] X. Liu,[31] Y. Liu,[31] Y. B. Liu,[36] Z. A. Liu,[1,49,54] Z. Q. Liu,[41] X. C. Lou,[1,49,54] F. X. Lu,[50] H. J. Lu,[18] J. D. Lu,[1,54] J. G. Lu,[1,49] X. L. Lu,[1] Y. Lu,[1] Y. P. Lu,[1,49] C. L. Luo,[34] M. X. Luo,[70] P. W. Luo,[50] T. Luo,[9,h] X. L. Luo,[1,49] X. R. Lyu,[54] F. C. Ma,[33] H. L. Ma,[1] L. L. Ma,[41] M. M. Ma,[1,54] Q. M. Ma,[1] R. Q. Ma,[1,54] R. T. Ma,[54] X. X. Ma,[1,54] X. Y. Ma,[1,49] F. E. Maas,[15] M. Maggiora,[66a,66c] S. Maldaner,[4] S. Malde,[61] Q. A. Malik,[65] A. Mangoni,[23b] Y. J. Mao,[38,k] Z. P. Mao,[1] S. Marcello,[66a,66c] Z. X. Meng,[57] J. G. Messchendorp,[55] G. Mezzadri,[24a] T. J. Min,[35] R. E. Mitchell,[22] X. H. Mo,[1,49,54] Y. J. Mo,[6] N. Yu. Muchnoi,[10,c] H. Muramatsu,[59] S. Nakhoul,[11,f] Y. Nefedov,[29] F. Nerling,[11,f] I. B. Nikolaev,[10,c] Z. Ning,[1,49] S. Nisar,[8,i] S. L. Olsen,[54] Q. Ouyang,[1,49,54] S. Pacetti,[23b,23c] X. Pan,[9,h] Y. Pan,[58] A. Pathak,[1] P. Patteri,[23a] M. Pelizaeus,[4] H. P. Peng,[63,49] K. Peters,[11,f] J. Pettersson,[67] J. L. Ping,[34] R. G. Ping,[1,54] R. Poling,[59] V. Prasad,[63,49] H. Qi,[63,49] H. R. Qi,[52] K. H. Qi,[25] M. Qi,[35] T. Y. Qi,[9] T. Y. Qi,[2] S. Qian,[1,49] W. B. Qian,[54] Z. Qian,[50] C. F. Qiao,[54] L. Q. Qin,[12] X. P. Qin,[9] X. S. Qin,[41] Z. H. Qin,[1,49] J. F. Qiu,[1] S. Q. Qu,[36] K. H. Rashid,[65] K. Ravindran,[21] C. F. Redmer,[28] A. Rivetti,[66c] V. Rodin,[55] M. Rolo,[66c] G. Rong,[1,54] Ch. Rosner,[15] M. Rump,[60] H. S. Sang,[63] A. Sarantsev,[29,d] Y. Schelhaas,[28] C. Schnier,[4] K. Schoenning,[67] M. Scodeggio,[24a,24b] D. C. Shan,[46] W. Shan,[19] X. Y. Shan,[63,49] J. F. Shangguan,[46] M. Shao,[63,49] C. P. Shen,[9] P. X. Shen,[36] X. Y. Shen,[1,54] H. C. Shi,[63,49] R. S. Shi,[1,54] X. Shi,[1,49] X. D. Shi,[63,49] J. J. Song,[41] W. M. Song,[27,1] Y. X. Song,[38,k] S. Sosio,[66a,66c] S. Spataro,[66a,66c] K. X. Su,[68] P. P. Su,[46] F. F. Sui,[41] G. X. Sun,[1] H. K. Sun,[1] J. F. Sun,[16] L. Sun,[68] S. S. Sun,[1,54] T. Sun,[1,54] W. Y. Sun,[34] W. Y. Sun,[27] X. Sun,[20,l] Y. J. Sun,[63,49] Y. K. Sun,[63,49] Y. Z. Sun,[1] Z. T. Sun,[1] Y. H. Tan,[68] Y. X. Tan,[63,49] C. J. Tang,[45] G. Y. Tang,[1] J. Tang,[50] J. X. Teng,[63,49] V. Thoren,[67] W. H. Tian,[43] Y. T. Tian,[25] I. Uman,[53b] B. Wang,[1] C. W. Wang,[35] D. Y. Wang,[38,k] H. J. Wang,[31] H. P. Wang,[1,54] K. Wang,[1,49] L. L. Wang,[1] M. Wang,[41] M. Z. Wang,[38,k] Meng Wang,[1,54] T. Wang,[12] W. Wang,[50] W. H. Wang,[68] W. P. Wang,[63,49] X. Wang,[38,k] X. F. Wang,[31] X. L. Wang,[9,h] Y. Wang,[50] Y. Wang,[63,49] Y. D. Wang,[37] Y. F. Wang,[1,49,54] Y. Q. Wang,[1] Y. Y. Wang,[31] Z. Wang,[1,49] Z. Y. Wang,[1] Ziyi Wang,[54] Zongyuan Wang,[1,54] D. H. Wei,[12] F. Weidner,[60] S. P. Wen,[1] D. J. White,[58] U. Wiedner,[4] G. Wilkinson,[61] M. Wolke,[67] L. Wollenberg,[4] J. F. Wu,[1,54] L. H. Wu,[1] L. J. Wu,[1,54] X. Wu,[9,h] Z. Wu,[1,49] L. Xia,[63,49] H. Xiao,[9,h] S. Y. Xiao,[1] Z. J. Xiao,[34] X. H. Xie,[38,k] Y. G. Xie,[1,49] Y. H. Xie,[6] T. Y. Xing,[1,54] G. F. Xu,[1] Q. J. Xu,[14] W. Xu,[1,54] X. P. Xu,[46] Y. C. Xu,[54] F. Yan,[9,h] L. Yan,[9,h] W. B. Yan,[63,49] W. C. Yan,[71] Xu Yan,[46] H. J. Yang,[42,g] H. X. Yang,[1] L. Yang,[43] S. L. Yang,[54] Y. X. Yang,[12] Yifan Yang,[1,54] Zhi Yang,[25] M. Ye,[1,49] M. H. Ye,[7] J. H. Yin,[1] Z. Y. You,[50] B. X. Yu,[1,49,54] C. X. Yu,[36] G. Yu,[1,54] J. S. Yu,[20,l] T. Yu,[64] C. Z. Yuan,[1,54] L. Yuan,[2] X. Q. Yuan,[38,k] Y. Yuan,[1] Z. Y. Yuan,[50] C. X. Yue,[32] A. Yuncu,[53a,a] A. A. Zafar,[65]

Y. Zeng,[20,l] B. X. Zhang,[1] Guangyi Zhang,[16] H. Zhang,[63] H. H. Zhang,[50] H. H. Zhang,[27] H. Y. Zhang,[1,49] J. J. Zhang,[43] J. L. Zhang,[69] J. Q. Zhang,[34] J. W. Zhang,[1,49,54] J. Y. Zhang,[1] J. Z. Zhang,[1,54] Jianyu Zhang,[1,54] Jiawei Zhang,[1,54] L. M. Zhang,[52] L. Q. Zhang,[50] Lei Zhang,[35] S. Zhang,[50] S. F. Zhang,[35] Shulei Zhang,[20,l] X. D. Zhang,[37] X. Y. Zhang,[41] Y. Zhang,[61] Y. H. Zhang,[1,49] Y. T. Zhang,[63,49] Yan Zhang,[63,49] Yao Zhang,[1] Yi Zhang,[9,h] Z. H. Zhang,[6] Z. Y. Zhang,[68] G. Zhao,[1] J. Zhao,[32] J. Y. Zhao,[1,54] J. Z. Zhao,[1,49] Lei Zhao,[63,49] Ling Zhao,[1] M. G. Zhao,[36] Q. Zhao,[1] S. J. Zhao,[71] Y. B. Zhao,[1,49] Y. X. Zhao,[25] Z. G. Zhao,[63,49] A. Zhemchugov,[29,b] B. Zheng,[64] J. P. Zheng,[1,49] Y. Zheng,[38,k] Y. H. Zheng,[54] B. Zhong,[34] C. Zhong,[64] L. P. Zhou,[1,54] Q. Zhou,[1,54] X. Zhou,[68] X. K. Zhou,[54] X. R. Zhou,[63,49] X. Y. Zhou,[32] A. N. Zhu,[1,54] J. Zhu,[36] K. Zhu,[1] K. J. Zhu,[1,49,54] S. H. Zhu,[62] T. J. Zhu,[69] W. J. Zhu,[9,h] W. J. Zhu,[36] Y. C. Zhu,[63,49] Z. A. Zhu,[1,54] B. S. Zou,[1] and J. H. Zou[1]

(BESIII Collaboration)

[1]*Institute of High Energy Physics, Beijing 100049, People's Republic of China*
[2]*Beihang University, Beijing 100191, People's Republic of China*
[3]*Beijing Institute of Petrochemical Technology, Beijing 102617, People's Republic of China*
[4]*Bochum Ruhr-University, D-44780 Bochum, Germany*
[5]*Carnegie Mellon University, Pittsburgh, Pennsylvania 15213, USA*
[6]*Central China Normal University, Wuhan 430079, People's Republic of China*
[7]*China Center of Advanced Science and Technology, Beijing 100190, People's Republic of China*
[8]*COMSATS University Islamabad, Lahore Campus, Defence Road, Off Raiwind Road, 54000 Lahore, Pakistan*
[9]*Fudan University, Shanghai 200443, People's Republic of China*
[10]*G.I. Budker Institute of Nuclear Physics SB RAS (BINP), Novosibirsk 630090, Russia*
[11]*GSI Helmholtzcentre for Heavy Ion Research GmbH, D-64291 Darmstadt, Germany*
[12]*Guangxi Normal University, Guilin 541004, People's Republic of China*
[13]*Guangxi University, Nanning 530004, People's Republic of China*
[14]*Hangzhou Normal University, Hangzhou 310036, People's Republic of China*
[15]*Helmholtz Institute Mainz, Staudinger Weg 18, D-55099 Mainz, Germany*
[16]*Henan Normal University, Xinxiang 453007, People's Republic of China*
[17]*Henan University of Science and Technology, Luoyang 471003, People's Republic of China*
[18]*Huangshan College, Huangshan 245000, People's Republic of China*
[19]*Hunan Normal University, Changsha 410081, People's Republic of China*
[20]*Hunan University, Changsha 410082, People's Republic of China*
[21]*Indian Institute of Technology Madras, Chennai 600036, India*
[22]*Indiana University, Bloomington, Indiana 47405, USA*
[23a]*INFN Laboratori Nazionali di Frascati, INFN Laboratori Nazionali di Frascati, I-00044 Frascati, Italy*
[23b]*INFN Sezione di Perugia, I-06100 Perugia, Italy*
[23c]*University of Perugia, I-06100 Perugia, Italy*
[24a]*INFN Sezione di Ferrara, INFN Sezione di Ferrara, I-44122 Ferrara, Italy*
[24a]*University of Ferrara, I-44122 Ferrara, Italy*
[25]*Institute of Modern Physics, Lanzhou 730000, People's Republic of China*
[26]*Institute of Physics and Technology, Peace Ave. 54B, Ulaanbaatar 13330, Mongolia*
[27]*Jilin University, Changchun 130012, People's Republic of China*
[28]*Johannes Gutenberg University of Mainz, Johann-Joachim-Becher-Weg 45, D-55099 Mainz, Germany*
[29]*Joint Institute for Nuclear Research, 141980 Dubna, Moscow region, Russia*
[30]*Justus-Liebig-Universitaet Giessen, II. Physikalisches Institut, Heinrich-Buff-Ring 16, D-35392 Giessen, Germany*
[31]*Lanzhou University, Lanzhou 730000, People's Republic of China*
[32]*Liaoning Normal University, Dalian 116029, People's Republic of China*
[33]*Liaoning University, Shenyang 110036, People's Republic of China*
[34]*Nanjing Normal University, Nanjing 210023, People's Republic of China*
[35]*Nanjing University, Nanjing 210093, People's Republic of China*
[36]*Nankai University, Tianjin 300071, People's Republic of China*
[37]*North China Electric Power University, Beijing 102206, People's Republic of China*
[38]*Peking University, Beijing 100871, People's Republic of China*
[39]*Qufu Normal University, Qufu 273165, People's Republic of China*
[40]*Shandong Normal University, Jinan 250014, People's Republic of China*
[41]*Shandong University, Jinan 250100, People's Republic of China*
[42]*Shanghai Jiao Tong University, Shanghai 200240, People's Republic of China*

[43]Shanxi Normal University, Linfen 041004, People's Republic of China
[44]Shanxi University, Taiyuan 030006, People's Republic of China
[45]Sichuan University, Chengdu 610064, People's Republic of China
[46]Soochow University, Suzhou 215006, People's Republic of China
[47]South China Normal University, Guangzhou 510006, People's Republic of China
[48]Southeast University, Nanjing 211100, People's Republic of China
[49]State Key Laboratory of Particle Detection and Electronics, Beijing 100049, Hefei 230026, People's Republic of China
[50]Sun Yat-Sen University, Guangzhou 510275, People's Republic of China
[51]Suranaree University of Technology, University Avenue 111, Nakhon Ratchasima 30000, Thailand
[52]Tsinghua University, Beijing 100084, People's Republic of China
[53a]Turkish Accelerator Center Particle Factory Group, Istanbul Bilgi University, 34060 Eyup, Istanbul, Turkey
[53a]Near East University, Nicosia, North Cyprus, Mersin 10, Turkey
[54]University of Chinese Academy of Sciences, Beijing 100049, People's Republic of China
[55]University of Groningen, NL-9747 AA Groningen, The Netherlands
[56]University of Hawaii, Honolulu, Hawaii 96822, USA
[57]University of Jinan, Jinan 250022, People's Republic of China
[58]University of Manchester, Oxford Road, Manchester M13 9PL, United Kingdom
[59]University of Minnesota, Minneapolis, Minnesota 55455, USA
[60]University of Muenster, Wilhelm-Klemm-Str. 9, 48149 Muenster, Germany
[61]University of Oxford, Keble Rd, Oxford OX13RH, United Kingdom
[62]University of Science and Technology Liaoning, Anshan 114051, People's Republic of China
[63]University of Science and Technology of China, Hefei 230026, People's Republic of China
[64]University of South China, Hengyang 421001, People's Republic of China
[65]University of the Punjab, Lahore-54590, Pakistan
[66a]University of Turin and INFN, University of Turin, I-10125 Turin, Italy
[66b]University of Eastern Piedmont, I-15121 Alessandria, Italy
[66c]INFN, I-10125 Turin, Italy
[67]Uppsala University, Box 516, SE-75120 Uppsala, Sweden
[68]Wuhan University, Wuhan 430072, People's Republic of China
[69]Xinyang Normal University, Xinyang 464000, People's Republic of China
[70]Zhejiang University, Hangzhou 310027, People's Republic of China
[71]Zhengzhou University, Zhengzhou 450001, People's Republic of China

(Received 31 March 2021; accepted 6 May 2021; published 9 June 2021)

Based on 4.481×10^8 $\psi(3686)$ events collected with the BESIII detector at BEPCII, the branching fraction of the isospin violating decay $\psi(3686) \to \bar{\Sigma}^0\Lambda + \text{c.c.}$ is measured to be $(1.60 \pm 0.31 \pm 0.13 \pm 0.58) \times 10^{-6}$, where the first uncertainty is statistical, the second is systematic, and the third is the uncertainty arising from interference with the continuum. This result is significantly

[a]Also at Bogazici University, 34342 Istanbul, Turkey.
[b]Also at the Moscow Institute of Physics and Technology, Moscow 141700, Russia.
[c]Also at the Novosibirsk State University, Novosibirsk, 630090, Russia.
[d]Also at the NRC "Kurchatov Institute", PNPI, 188300, Gatchina, Russia.
[e]Also at Istanbul Arel University, 34295 Istanbul, Turkey.
[f]Also at Goethe University Frankfurt, 60323 Frankfurt am Main, Germany.
[g]Also at Key Laboratory for Particle Physics, Astrophysics and Cosmology, Ministry of Education; Shanghai Key Laboratory for Particle Physics and Cosmology; Institute of Nuclear and Particle Physics, Shanghai 200240, People's Republic of China.
[h]Also at Key Laboratory of Nuclear Physics and Ion-beam Application (MOE) and Institute of Modern Physics, Fudan University, Shanghai 200443, People's Republic of China.
[i]Also at Harvard University, Department of Physics, Cambridge, Massachusetts 02138, USA.
[j]Currently at: Institute of Physics and Technology, Peace Ave. 54B, Ulaanbaatar 13330, Mongolia.
[k]Also at State Key Laboratory of Nuclear Physics and Technology, Peking University, Beijing 100871, People's Republic of China.
[l]School of Physics and Electronics, Hunan University, Changsha 410082, China.
[m]Also at Guangdong Provincial Key Laboratory of Nuclear Science, Institute of Quantum Matter, South China Normal University, Guangzhou 510006, China.

Published by the American Physical Society under the terms of the Creative Commons Attribution 4.0 International license. Further distribution of this work must maintain attribution to the author(s) and the published article's title, journal citation, and DOI. Funded by SCOAP^3.

smaller than the measurement based on CLEO-c data sets. The decays $\chi_{cJ} \to \Lambda\bar{\Lambda}$ are measured via $\psi(3686) \to \gamma\chi_{cJ}$, and the branching fractions are determined to be $\mathcal{B}(\chi_{c0} \to \Lambda\bar{\Lambda}) = (3.64 \pm 0.10 \pm 0.10 \pm 0.07) \times 10^{-4}$, $\mathcal{B}(\chi_{c1} \to \Lambda\bar{\Lambda}) = (1.31 \pm 0.06 \pm 0.06 \pm 0.03) \times 10^{-4}$, $\mathcal{B}(\chi_{c2} \to \Lambda\bar{\Lambda}) = (1.91 \pm 0.08 \pm 0.17 \pm 0.04) \times 10^{-4}$, where the third uncertainties are systematic due to the $\psi(3686) \to \gamma\chi_{cJ}$ branching fractions.

DOI: 10.1103/PhysRevD.103.112004

I. INTRODUCTION

Experimental studies of charmonium decays are essential for understanding the structures and decay mechanisms of charmonium states. These measurements enable tests of nonperturbative quantum chromodynamics (QCD) models. Further, charmonium decays to baryon pairs provide a novel method to explore the properties of baryons [1,2]. In recent years, there have been searches for missing decays and measurements of angular distributions and polarizations of many J/ψ and $\psi(3686)$ two-body decays to baryon and antibaryon final states with much improved precision by the CLEO, BESII, and BESIII collaborations [3–14]. In addition, these measurements also provide the possibility to determine the relative phase between strong and electromagnetic amplitudes [15].

In spite of the significant improvements achieved on J/ψ and $\psi(3686)$ decays into baryon pairs, information on isospin symmetry breaking decays is still limited due to their low decay rates. Recently, a measurement of the isospin violating decay $\psi(3686) \to \bar{\Sigma}^0\Lambda + \text{c.c.}$ is reported and obtained a branching fraction of $\mathcal{B}(\psi(3686) \to \bar{\Sigma}^0\Lambda + \text{c.c.}) = (12.3 \pm 2.4) \times 10^{-6}$ based on $2.45 \times 10^7 \psi(3686)$ decay events collected with CLEO-c detector [16]. This result is much larger than theoretical predictions [15], and a specific mechanism is proposed by the authors of [17] to explain its abnormal largeness. In our analysis, we use a sample of 4.481×10^8 $\psi(3686)$ events collected at BESIII to measure the branching fraction of $\psi(3686) \to \bar{\Sigma}^0\Lambda + \text{c.c.}$, with $\bar{\Sigma}^0 \to \gamma\bar{\Lambda}$, $\bar{\Lambda}(\Lambda) \to \bar{p}\pi^+(p\pi^-)$.

With the same final states, we can also study the $\Lambda\bar{\Lambda}$ pair decay from the P-wave charmonium χ_{cJ} states, which are produced via a radiative transition from the $\psi(3686)$. Using $1.068 \times 10^8 \psi(3686)$ events collected in 2009, BESIII previously reported the branching-fraction measurements of $\mathcal{B}(\chi_{c0} \to \Lambda\bar{\Lambda}) = (33.3 \pm 2.0 \pm 2.6) \times 10^{-5}$ $\mathcal{B}(\chi_{c1} \to \Lambda\bar{\Lambda}) = (12.2 \pm 1.1 \pm 1.1) \times 10^{-5}$, and $\mathcal{B}(\chi_{c2} \to \Lambda\bar{\Lambda}) = (20.8 \pm 1.6 \pm 2.3) \times 10^{-5}$ [18].

II. DETECTOR AND MONTE CARLO SIMULATION

The BESIII detector [19] records symmetric e^+e^- collisions provided by the BEPCII storage ring [20], which operates with a peak luminosity of 1×10^{33} cm^{-2} s^{-1} in the center-of-mass energy range from 2.0 to 4.7 GeV. BESIII has collected large data samples in this energy region [21]. The cylindrical core of the BESIII detector covers 93% of the full solid angle and consists of a helium-based multilayer drift chamber (MDC), a plastic scintillator time-of-flight system (TOF), and a CsI(Tl) electromagnetic calorimeter (EMC), which are all enclosed in a superconducting solenoidal magnet providing a 1.0 T magnetic field. The solenoid is supported by an octagonal flux-return yoke with resistive plate counter muon identification modules interleaved with steel. The acceptance of charged particles and photons is 93% of the 4π solid angle. The charged-particle momentum resolution at 1 GeV$/c$ is 0.5%, and the dE/dx resolution is 6% for electrons from Bhabha scattering. The EMC measures photon energies with a resolution of 2.5% (5%) at 1 GeV in the barrel (end cap) region. The time resolution in the TOF barrel region is 68 ps, while that in the end cap region is 110 ps.

Simulated Monte Carlo (MC) samples produced with GEANT4-based [22] software, which includes the geometric description of the BESIII detector and the detector response, are used to determine detection efficiencies, estimate background contributions, and study systematic uncertainties. The simulation models the beam energy spread and initial state radiation (ISR) in the e^+e^- annihilations with the generator KKMC [23]. The inclusive MC sample simulates every possible process, who includes the production of the $\psi(3686)$ resonance, the ISR production of the J/ψ, and the continuum processes incorporated in KKMC [23]. The known decay modes are modeled with EVTGEN [24] using branching fractions taken from the Particle Data Group [25], and the remaining unknown charmonium decays are modeled with LUNDCHARM [26]. Final state radiation (FSR) from charged particles is incorporated using PHOTOS [27]. For the signal processes, we use MC samples of $\psi(3686) \to \bar{\Sigma}^0\Lambda + \text{c.c.}$ decays generated with uniform phase space (PHSP), while $\psi(3686) \to \gamma\chi_{cJ}$ decays are generated according to helicity amplitudes [28] and $\chi_{cJ} \to \Lambda\bar{\Lambda}$ with PHSP.

III. $\psi(3686) \to \bar{\Sigma}^0\Lambda + \text{c.c.}$

A. Event selection

Since the final state of interest is $\gamma p\bar{p}\pi^+\pi^-$, we require each $\psi(3686)$ candidate to contain four charged tracks with zero net charge and at least one photon. Each charged track, detected in the MDC is required to satisfy $|\cos\theta| < 0.93$, where θ is defined with respect to the z-axis, which is the symmetry axis of the MDC. The distance of closest approach to the interaction point (IP) must be less than 30 cm along the z-axis, and less than 10 cm in the transverse plane. Pions and protons are identified by the magnitude of their momentum, and charged tracks with momentum larger than 0.7 GeV$/c$ in the lab frame are identified as protons. Other tracks are identified as pions. An isolated cluster in the EMC is considered to be a photon if the following requirements are satisfied: 1) the deposited energy of each shower must be more than 25 MeV in the barrel region ($|\cos\theta| < 0.80$) and more than 50 MeV in the end cap region ($0.86 < |\cos\theta| < 0.92$); 2) to suppress electronic noise and showers unrelated to the event, the difference between the EMC time and the event start time is required to be within (0, 700) ns; 3) to exclude showers that originate from charged tracks, the angle between the position of each shower in the EMC and the closest extrapolated charged track of p, π^+, or π^- must be greater than 10 degrees, and greater than 20 degrees for the $\bar{p}$ track.

The $\Lambda(\bar{\Lambda})$ candidate is reconstructed with any $p\pi^-$ ($\bar{p}\pi^+$) combination satisfying a secondary vertex fit [29]. The secondary vertex fit is required to be successful, but no additional requirements are placed on the fit χ^2. To improve the momentum and energy resolution and to reduce background contributions, a six-constraint (6C) kinematic fit is applied to the event candidates with constraints on the total four-momentum and the invariant masses of the Λ and $\bar{\Lambda}$ candidates. The χ^2_{6C} of the kinematic fit is required to be less than 25.

To further suppress background, we require: 1) the χ^2_{6C} for the $\gamma p\bar{p}\pi^+\pi^-$ hypothesis is less than those for any $\gamma\gamma p\bar{p}\pi^+\pi^-$ or $p\bar{p}\pi^+\pi^-$ hypothesis: $\chi^2_{\gamma p\bar{p}\pi^+\pi^-} < \chi^2_{\gamma\gamma p\bar{p}\pi^+\pi^-}$, $\chi^2_{\gamma p\bar{p}\pi^+\pi^-} < \chi^2_{p\bar{p}\pi^+\pi^-}$; 2) the $\Lambda(\bar{\Lambda})$ lifetime must satisfy $L_{\Lambda(\bar{\Lambda})}/\sigma > 2$ where L and σ are the decay length and its uncertainty obtained from the secondary vertex fit; 3) the invariant mass of the $\Lambda\bar{\Lambda}$, $M_{\Lambda\bar{\Lambda}}$ is required to be greater than 3.48 GeV$/c^2$ in order to suppress the $\psi(3686) \to \gamma\chi_{c0}, \chi_{c0} \to \Lambda\bar{\Lambda}$ background; 4) $M_{\gamma\Lambda} > 1.15$ GeV$/c^2$ and $\gamma_{\bar{\Lambda}} > 1.15$ GeV$/c^2$ are required to suppress background from $\psi(3686) \to \Lambda\bar{\Lambda}$.

After imposing the above requirements, Fig. 1 shows the scatter plots of $M_{\gamma\bar{\Lambda}}$ versus $M_{\gamma\Lambda}$ for data, inclusive MC samples, and signal MC samples of $\psi(3686) \to \bar{\Sigma}^0\Lambda$ and $\psi(3686) \to \Sigma^0\bar{\Lambda}$ processes. The $\psi(3686) \to \bar{\Sigma}^0\Lambda$ + c.c. signals are clearly visible in Fig. 1(a). The two sloped bands are backgrounds from $\psi(3686) \to \gamma\chi_{c1,2}$, $\chi_{c1,2} \to \Lambda\bar{\Lambda}$, which are well simulated by the inclusive

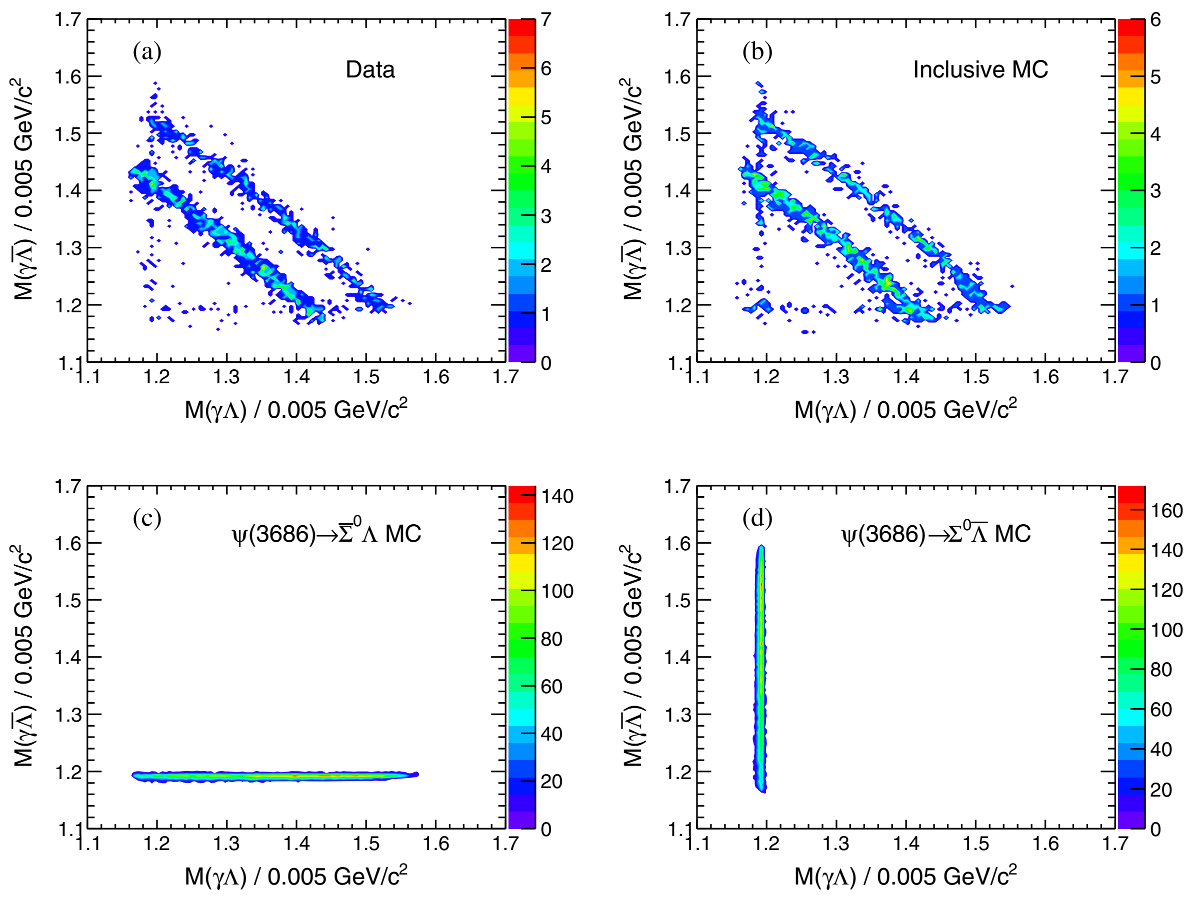

FIG. 1. Scatter distributions of $M_{\gamma\bar{\Lambda}}$ versus $M_{\gamma\Lambda}$ at the $\psi(3686)$ resonance. (a)–(d) are distributions from data, inclusive MC samples, and signal MC samples of $\psi(3686) \to \bar{\Sigma}^0\Lambda$ and $\psi(3686) \to \Sigma^0\bar{\Lambda}$ decays, respectively.

MC samples as shown in Fig. 1(b). The inclusive MC indicates that the only peaking background is from $\psi(3686) \to \bar{\Sigma}^0\Sigma^0$. Figures 1(c) and 1(d) are the signal shapes of $\psi(3686) \to \bar{\Sigma}^0\Lambda$ and $\psi(3686) \to \Sigma^0\bar{\Lambda}$, which are vertical and horizonal bands in the scatter plot distributions, respectively.

B. Signal yields and branching fraction calculation

We determine the signal yields by an unbinned maximum-likelihood fit to the two-dimensional distributions of the $\gamma\Lambda$ and $\gamma\bar{\Lambda}$ invariant masses. The signal shapes are determined from signal MC simulation for the $\Sigma^0\bar{\Lambda}$ and $\bar{\Sigma}^0\Lambda$ processes. The background shape includes five items: $\psi(3686) \to \Sigma^0\bar{\Sigma}^0$, $\psi(3686) \to \gamma\chi_{cJ}(\chi_{cJ} \to \Lambda\bar{\Lambda})$ with $J = 0$, 1, 2, and other background contributions. The shapes of the first four items are determined from MC simulation while the last one is described by a two-variable first-order polynomial function $f(m_{\gamma\Lambda}, m_{\gamma\bar{\Lambda}}) = am_{\gamma\Lambda} + bm_{\gamma\bar{\Lambda}} + c$ where a, b, c are constant parameters that are determined in the fit. The background yields are floated in the fit except the peaking background $\psi(3686) \to \Sigma^0\bar{\Sigma}^0$ which is included with its magnitude determined from previous measurements [16]. The χ_{cJ} background yields are consistent with expectation after considering branching fractions [25] and efficiencies. Figure 2 shows the projections of the two-dimensional fitting results. The numbers of signal events are determined to be $N^{\mathrm{sig}}_{\gamma\bar{\Lambda}} = 26.1 \pm 6.6$, $N^{\mathrm{sig}}_{\gamma\Lambda} = 37.2 \pm 7.7$ from the fit.

The contribution from the continuum process, i.e., $e^+e^- \to \gamma^* \to \bar{\Sigma}^0\Lambda + \mathrm{c.c.}$, is estimated from the collision data at 3.773 GeV with integrated luminosity of 2931.8 pb^{-1} taken during 2010 and 2011. The same event selection criteria as for the $\psi(3686) \to \bar{\Sigma}^0\Lambda + \mathrm{c.c.}$ decay is applied. In addition, $|\mathrm{M}_{\Lambda\bar{\Lambda}} - 3.686\ \mathrm{GeV}/c^2| > 0.01\ \mathrm{GeV}/c^2$ is required to suppress background from the $e^+e^- \to \gamma_{\mathrm{ISR}}\ \psi(3686)$, $\psi(3686) \to \Lambda\bar{\Lambda}$ process. An unbinned one-dimensional maximum-likelihood fit is done to determine signal yields, where the peaking background $e^+e^- \to \bar{\Sigma}^0\Sigma^0$ has been considered with its shape from MC simulation and magnitude from previous measurements [16]. The other backgrounds are described with a second-order polynomial function. To account for the difference of the integrated luminosity and cross sections between the two energy points 3.686 GeV and 3.773 GeV, a scaling factor $f = 0.24$ is applied. The continuum contributions at 3.686 GeV are determined to be: $N^{\mathrm{cont}}_{\gamma\bar{\Lambda}} = 6.2 \pm 1.2$ and $N^{\mathrm{cont}}_{\gamma\Lambda} = 3.9 \pm 1.0$ in the $\Sigma^0\bar{\Lambda}$ and $\bar{\Sigma}^0\bar{\Lambda}$ processes, respectively, where the contributions from $e^+e^- \to \psi(3770) \to \bar{\Sigma}^0\Lambda + \mathrm{c.c.}$ decay have been ignored due to its low production.

The branching fraction of $\psi(3686) \to \bar{\Sigma}^0\Lambda$ is calculated by

$$\mathcal{B}(\psi(3686) \to \bar{\Sigma}^0\Lambda) = \frac{N^{\mathrm{sig}}_{\gamma\bar{\Lambda}} - N^{\mathrm{cont}}_{\gamma\bar{\Lambda}}}{N_{\psi(3686)} \cdot \epsilon_{\bar{\Sigma}^0\Lambda} \cdot \mathrm{Br}}. \tag{1}$$

Here, $N_{\psi(3686)}$ is the total number of $\psi(3686)$ events [30], $\mathrm{Br} = \mathcal{B}(\bar{\Lambda} \to \bar{p}\pi^+) \cdot \mathcal{B}(\Lambda \to p\pi^-) \cdot \mathcal{B}(\bar{\Sigma}^0 \to \gamma\bar{\Lambda})$ [25], and the efficiency $\epsilon_{\bar{\Sigma}^0\Lambda} = 16.52\%$ is determined from simulation. The branching fraction of $\psi(3686) \to \bar{\Sigma}^0\Lambda$ is determined to be $(0.66 \pm 0.22) \times 10^{-6}$. Similarly, the branching fraction of $\psi(3686) \to \Sigma^0\bar{\Lambda}$ is calculated to be $(0.94 \pm 0.22) \times 10^{-6}$, with $\epsilon_{\Sigma^0\bar{\Lambda}} = 19.44\%$. The clear difference between $\epsilon_{\Sigma^0\bar{\Lambda}}$ and $\epsilon_{\bar{\Sigma}^0\Lambda}$ comes from the different selection criteria on the open angle between photon and (anti)proton. The combined branching fraction of $\psi(3686) \to \bar{\Sigma}^0\Lambda + \mathrm{c.c.}$ is $\mathcal{B}(\psi(3686) \to \bar{\Sigma}^0\Lambda + \mathrm{c.c.}) = (1.60 \pm 0.31) \times 10^{-6}$, where the uncertainty is statistical only.

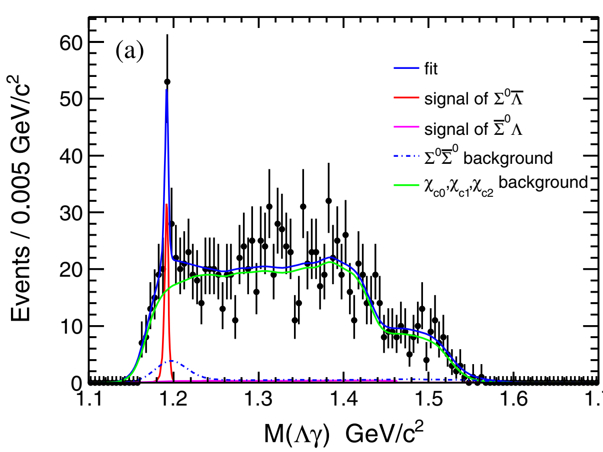

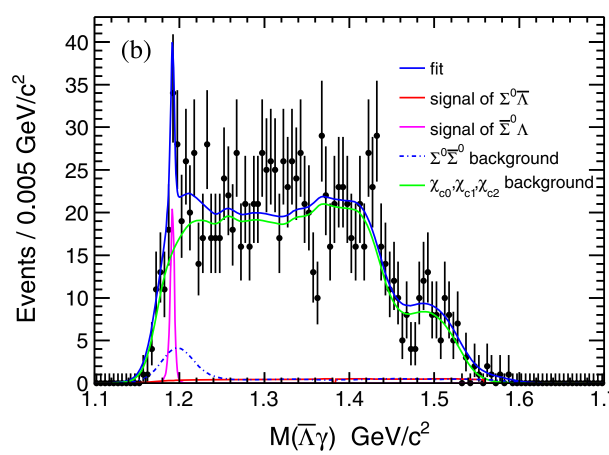

FIG. 2. The projections from the two-dimensional fit to $\mathrm{M}_{\gamma\Lambda}$ and $\mathrm{M}_{\gamma\bar{\Lambda}}$. Dots with error bars are data, blue solid curves are fitting results, red and pink curves are the signals, blue dotted lines are from normalized $\psi(3686) \to \bar{\Sigma}^0\Sigma^0$ background contributions, green lines show the $\psi(3686) \to \gamma\chi_{cJ}$ background contributions, the contributions from other backgrounds are too small to be drawn on the plots.

C. Systematic uncertainties

The systematic uncertainties on the branching-fraction measurement include those from track and photon reconstruction efficiencies, kinematic fit, angle requirement, $\Lambda(\bar{\Lambda})$ reconstruction efficiency, signal and background shapes, and the branching fraction of $\Lambda(\bar{\Lambda})$ decay.

The uncertainty due to photon detection efficiency is 1% per photon, which is determined from a study of the control sample $J/\psi \to \rho\pi$ [31].

The efficiency of $\Lambda(\bar{\Lambda})$ reconstruction is studied using the control sample of $\psi(3686) \to \Lambda\bar{\Lambda}$ decays, and a correction factor 0.980 ± 0.011 [32] is applied to the efficiencies obtained from MC simulation. The uncertainty of the correction factor, 1.1% already includes the uncertainties of MDC tracking and $\Lambda(\bar{\Lambda})$ reconstruction, and 1.1% is taken as the uncertainty of the efficiency of $\Lambda(\bar{\Lambda})$ reconstruction.

To study the uncertainty caused by the requirement on the angle between the position of each shower in the EMC and the closest extrapolated charged track, we utilize the processes $\psi(3686) \to \gamma\chi_{cJ}, \chi_{cJ} \to \Lambda\bar{\Lambda}$ due to their large statistics. Two sets of branching fractions are obtained. One is with the nominal requirement, i.e., the angle of each shower is at least 10° away from p, π^+, π^- tracks and 20° away from $\bar{p}$ track; the other one requires the angle of each shower to be at least 20° away from p, π^+, π^- tracks and 30° away from $\bar{p}$ track. The difference of the branching fractions obtained with the nominal and modified requirements is 1.6%, which is taken as the associated systematic uncertainty.

To study the uncertainty associated with the kinematic fit, the track helix parameters are corrected in the MC simulation [33]. The resulting 0.3% efficiency difference before and after the correction is taken as the systematic uncertainty related to the kinematic fit.

The systematic uncertainty associated with the signal shape is mainly due to the resolution difference between data and MC simulation. It is estimated by smearing the signal shape with a resolution of 5% of the one determined from MC simulation according to the study using the control sample of $\psi(3686) \to \bar{\Sigma}^0\Sigma^0$. The difference is 0.4% and is taken as the corresponding systematic uncertainty due to the signal shape.

For the peaking background, we fixed the shape and number of events in the fitting. We vary the number of background events by its uncertainty. A difference of 1.9% is assigned as systematic uncertainty.

The uncertainty associated with the χ_{c0}, χ_{c1}, and χ_{c2} backgrounds is estimated by fixing their contributions to the world average values [25] instead of floating them in the nominal fit. The differences between fixing and floating are 0.7%, 0.4%, and 2.1% for χ_{c0}, χ_{c1}, and χ_{c2}, respectively, and are taken as the systematic uncertainties.

The systematic uncertainty for the description of the other background contributions is estimated by changing from a two-variable first-order polynomial to a two-variable second-order polynomial to describe the shape of the other backgrounds. The systematic uncertainty is determined to be 0.1%.

TABLE I. Systematic uncertainties for the branching fraction of $\psi(3686) \to \bar{\Sigma}^0\Lambda + \text{c.c.}$ decay.

Source	$\psi(3686) \to \bar{\Sigma}^0\Lambda + \text{c.c.}(\%)$
Photon efficiency	1.0
Λ efficiency correction	1.1
Angle requirement	1.6
Kinematic fit	0.3
Signal shape	0.4
Peaking background	1.9
Background of $\psi(3686) \to \gamma\chi_{c0}$	0.7
Background of $\psi(3686) \to \gamma\chi_{c1}$	0.4
Background of $\psi(3686) \to \gamma\chi_{c2}$	2.1
Other nonresonance background	0.1
Physics model	6.9
$\mathcal{B}(\Lambda \to p\pi)$	1.1
Number of $\psi(3686)$	0.6
Total	7.9

In the signal MC sample, $\psi(3686) \to \bar{\Sigma}^0\Lambda + \text{c.c.}$ is simulated with a uniform distribution over phase space. However, the angular distribution should be described as $\mathrm{d}N/\mathrm{d}\cos\theta \propto 1 + \alpha\cos^2\theta$ [34] where θ is the polar angle of the (anti)baryon. Since the observed number of events does not allow the determination of the angular distribution in our analysis, we generate MC samples with $\alpha = -1.0$ and $\alpha = 1.0$, the two extreme scenarios. The efficiency difference between them is divided by $\sqrt{12}$ under the assumption that the prior distribution of α is uniform, and the result 6.9% is taken as the uncertainty associated to the angular distribution.

The uncertainty on the total number of $\psi(3686)$ events is 0.6% [30]. The uncertainty of the Λ decay branching fraction is taken from the world average value [25]. Table I lists all sources and values of systematic uncertainties, and the total systematic uncertainty is determined by adding them in quadrature.

D. Discussion and result

So far, we have not considered possible interference between the $\psi(3686)$ decay and the continuum process, which is described by

$$|A_{\text{cont}} + e^{i\theta}A_{\psi'}|^2 \propto N^{\text{sig}}_{\gamma\bar{\Lambda}}(N^{\text{sig}}_{\gamma\Lambda}), \tag{2}$$

where $A_{\psi'}$ and A_{cont} are the amplitudes of $\psi(3686) \to \bar{\Sigma}^0\Lambda + \text{c.c.}$ and the continuum contribution, respectively. The difference between $\theta = 0°$ and $\theta = 180°$, corresponding to the extreme constructive and destructive cases, respectively, is adopted as the uncertainty associated with

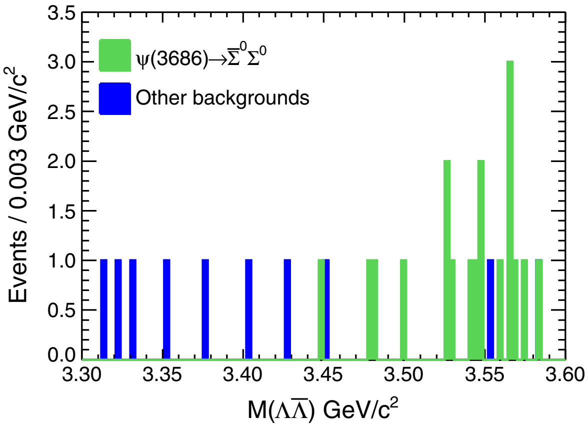

FIG. 3. The $\chi_{cJ} \to \Lambda\bar{\Lambda}$ background distributions from the inclusive MC samples. The green histogram is the $\Sigma^0\bar{\Sigma}^0$ background, and the blue one is all the other background contributions.

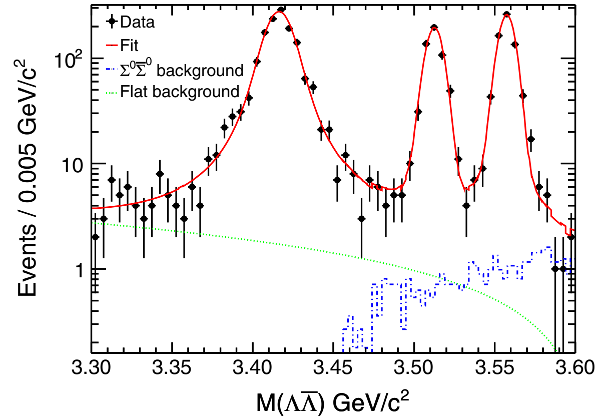

FIG. 4. Fitting results of the $\Lambda\bar{\Lambda}$ invariant mass distribution. Dots with error bars are data, the red solid line is the fitting curve, the blue dashed line is $\Sigma^0\bar{\Sigma}^0$ background, and the green dashed line is all other background contributions.

the interference. This difference is divided by $\sqrt{12}$, since the prior distribution of the interference angle is assumed to be uniform. Finally, the branching fractions are $\mathcal{B}(\psi(3686) \to \Sigma^0\bar{\Lambda}) = (0.94 \pm 0.39) \times 10^{-6}$ and $\mathcal{B}(\psi(3686) \to \bar{\Sigma}^0\Lambda) = (0.66 \pm 0.49) \times 10^{-6}$, where the uncertainties are only the systematic arising from interference. The combined branching fraction of $\psi(3686) \to \bar{\Sigma}^0\Lambda + \mathrm{c.c.}$ is $\mathcal{B}(\psi(3686) \to \bar{\Sigma}^0\Lambda + \mathrm{c.c.}) = (1.60 \pm 0.31 \pm 0.13 \pm 0.58) \times 10^{-6}$, where the first uncertainty is statistic, the second is systematic, and the third is the uncertainty due to interference with the continuum.

IV. $\chi_{cJ} \to \Lambda\bar{\Lambda}$

A. Event selection and background study

The initial selection criteria for charged tracks and photons and the $\Lambda(\bar{\Lambda})$ reconstruction are the same as those described above for $\psi(3686) \to \bar{\Sigma}^0\Lambda + \mathrm{c.c.}$. Additional selection criteria are 1) the χ^2 from the 6C kinematic fit is required to be less than 50, and 2) to veto $\psi(3686) \to \Sigma^0\bar{\Sigma}^0$ background, the $\gamma\Lambda(\gamma\bar{\Lambda})$ combination is required to be outside of the $\Sigma^0(\bar{\Sigma}^0)$ region, that is defined as within 12 MeV to the Σ^0 nominal mass [25]. The χ_{c0} veto is also removed.

After all selection requirements have been applied, Fig. 3 shows all background contributions according to the inclusive MC sample, which include two parts: nonflat $\Sigma^0\bar{\Sigma}^0$ background contributions that tend to accumulate in the χ_{c2} region and flat non-Σ^0 background contributions. Both background levels are quite low compared with the signal.

B. Signal yields and branching fractions

To determine the χ_{cJ} signal yields, we fit the $\Lambda\bar{\Lambda}$ invariant mass distribution with an unbinned maximum likelihood fit. Each χ_{cJ} signal shape is described by a Breit-Wigner function convolved with a Gaussian function, and the parameters of the Breit-Wigner functions are fixed to the world average values [25]. The Gaussian function represents the resolutions, whose parameters are floated in the fit but shared with all three χ_{cJ} resonances. The background shape is composed of two parts: a MC simulation of $\psi(3686) \to \Sigma^0\bar{\Sigma}^0$ events with both shape and number fixed and a second-order polynomial with floating parameters to describe other background contributions. The results are shown in Fig. 4. The amount of other backgrounds from the fit is obvious larger than that simulated in inclusive MC as shown in Fig. 3. It indicates the inclusive MC simulation is not perfect yet. The fitted χ_{cJ} signal yields are $N_{\chi_{c0}} = 1486 \pm 42$, $N_{\chi_{c1}} = 528 \pm 24$, $N_{\chi_{c2}} = 670 \pm 27$.

The product branching fractions of $\mathcal{B}(\chi_{cJ} \to \Lambda\bar{\Lambda}) \cdot \mathcal{B}(\psi(3686) \to \gamma\chi_{cJ})$ are determined by

$$\mathcal{B}(\chi_{cJ} \to \Lambda\bar{\Lambda}) \cdot \mathcal{B}(\psi(3686) \to \gamma\chi_{cJ}) = \frac{N_{\chi_{cJ}}}{N_{\psi(3686)} \cdot \epsilon \cdot \mathcal{B}(\Lambda \to p\pi^-) \cdot \mathcal{B}(\bar{\Lambda} \to \bar{p}\pi^+)}, \quad (3)$$

where ϵ is the efficiency. We calculate the branching fractions of $\chi_{cJ} \to \Lambda\bar{\Lambda}$ decays based on world averaged values of $\mathcal{B}(\psi(3686) \to \gamma\chi_{cJ})$ [25]. The results are listed in Table III.

C. Systematic uncertainties

The uncertainties in the branching-fraction measurement include photon and $\Lambda(\bar{\Lambda})$ reconstruction efficiencies, kinematic fit, signal and background shapes, fitting range, and the branching fraction of $\Lambda(\bar{\Lambda})$ decay.

The uncertainties due to the photon detection and $\bar{\Lambda}$ reconstruction efficiencies, the requirement on the angle between the position of each shower in the EMC and the

TABLE II. Systematic uncertainties of the branching fractions for $\chi_{cJ} \to \Lambda\bar{\Lambda}$ decays.

Source	$\chi_{c0}(\%)$	$\chi_{c1}(\%)$	$\chi_{c2}(\%)$
Photon efficiency	1.0	1.0	1.0
Λ efficiency correction	1.1	1.1	1.1
Kinematic fit	0.5	0.8	0.8
Angle requirement	1.6	1.6	1.6
Signal shape	0.6	0.3	0.1
Peaking background	0.0	0.2	0.4
Fitting range	0.6	1.8	0.7
Angular distribution	0.0	3.0	8.7
$\mathcal{B}(\Lambda \to p\pi)$	1.1	1.1	1.1
Number of $\psi(3686)$	0.6	0.6	0.6
Sum	2.7	4.4	9.1
$\mathcal{B}(\psi(3686) \to \gamma\chi_{cJ})$	2.0	2.5	2.1
Total	3.4	5.1	9.4

closest extrapolated charged tracks, the Λ branching fraction, and the number of $\psi(3686)$ events are the same as in the study of $\psi(3686) \to \bar{\Sigma}^0\Lambda + \text{c.c.}$, while that due to the kinematic fit is calculated in the same manner.

For the signal shapes, the single Gaussian is changed to a double Gaussian, and the differences in the yields of signal events, 0.6%, 0.3%, and 0.1% for χ_{c0}, χ_{c1}, and χ_{c2}, respectively, are taken as the systematic uncertainties associated with the signal shapes. We study the uncertainty associated with other background shapes by changing description from the second-order polynomial function to the third-order polynomial function. It turns out the difference is negligible.

The uncertainty associated with the fitting range is estimated by varying it from [3.30, 3.60] GeV to [3.32, 3.62] GeV. The differences 0.6%, 1.8%, and 0.7% for χ_{c0}, χ_{c1}, and χ_{c2} are taken as the uncertainty due to the fitting range.

The angular distributions of $\psi(3686) \to \gamma\chi_{c1,2}$ are known. However, knowledge of the $\chi_{c1,2} \to \Lambda\bar{\Lambda}$ angular distributions is still limited. We generate signal MC samples with a uniform distribution over phase space. To estimate the uncertainty caused by the angular distribution, we adopt the method used in Ref. [18]. We regenerate the signal MC samples according to the helicity amplitudes $B_{\lambda_3,\bar{\lambda}_3}$ defined in Ref. [28], where $\lambda_3(\bar{\lambda}_3)$ is the helicity of $\Lambda(\bar{\Lambda})$ in the rest frame of χ_{cJ}. The amplitudes $B_{\frac{1}{2},\frac{1}{2}}$ and $B_{\frac{1}{2},-\frac{1}{2}}$ are both set to be 1.0 to obtain the efficiency again, and the differences of 3.0% and 8.7% between these two models are taken as the associated systematic uncertainties.

Table II lists all sources of systematic uncertainty and the values for each decay channel. The total systematic uncertainties are determined by adding each contribution in quadrature.

D. Result

The branching fractions, compared with the world averaged values, are listed in Table III, where the third uncertainties for $\mathcal{B}(\chi_{cJ} \to \Lambda\bar{\Lambda})$ are the uncertainties due to the branching fractions of $\psi(3686) \to \gamma\chi_{cJ}$.

V. SUMMARY

The branching fraction of the isospin symmetry breaking decay $\psi(3686) \to \bar{\Sigma}^0\Lambda + \text{c.c.}$ is measured to be $\mathcal{B}(\psi(3686) \to \bar{\Sigma}^0\Lambda + \text{c.c.}) = (1.60 \pm 0.31 \pm 0.13 \pm 0.58) \times 10^{-6}$, where the first uncertainty is statistical, the second is systematic, the third one is the uncertainty due to interference with the continuum. Compared with the result using CLEO-c data [16], $(12.3 \pm 2.4) \times 10^{-6}$, our result is significantly smaller. Our measurement is consistent with the theoretical prediction [15], $(4.0 \pm 2.3) \times 10^{-6}$, within 1σ. However our branching fraction is measured under the assumption of no interference which corresponds to an angle of $\theta = 90°$, while the angle is assumed to be $0°$ in Ref. [15]. If $\theta = 0°$ is adopted, the branching fraction is measured to be $\mathcal{B}(\psi(3686) \to \bar{\Sigma}^0\Lambda + \text{c.c.}) = (1.02 \pm 0.31 \pm 0.13) \times 10^{-6}$, and the difference between our measurement and the theoretical prediction is larger than 1σ but still smaller than 2σ.

With the increased data sample collected at the BESIII detector, the branching fractions of $\chi_{cJ} \to \Lambda\bar{\Lambda}$ are measured via $\psi(3686) \to \gamma\chi_{cJ}$ with improved precision. The branching fractions are determined to be $\mathcal{B}(\chi_{c0} \to \Lambda\bar{\Lambda}) = (3.64 \pm 0.10 \pm 0.10 \pm 0.07) \times 10^{-4}$, $\mathcal{B}(\chi_{c1} \to \Lambda\bar{\Lambda}) = (1.31 \pm 0.06 \pm 0.06 \pm 0.03) \times 10^{-4}$, $\mathcal{B}(\chi_{c2} \to \Lambda\bar{\Lambda}) = (1.91 \pm 0.08 \pm 0.17 \pm 0.04) \times 10^{-4}$, where the first and second uncertainties are statistical and systematic, and the third ones are the systematic

TABLE III. The number of observed events $N_{\chi_{cJ}}$, efficiencies (ϵ), product branching fractions, and the branching fractions of $\chi_{cJ} \to \Lambda\bar{\Lambda}$ decays compared with the world average values, where the third uncertainties for $\mathcal{B}(\chi_{cJ} \to \Lambda\bar{\Lambda})$ are the uncertainties due to the branching fractions of $\psi(3686) \to \gamma\chi_{cJ}$ decays.

Mode	$N_{\chi_{cJ}}$	ϵ	$\mathcal{B}(\psi(3686) \to \gamma\chi_{cJ})$ $\times\mathcal{B}(\chi_{cJ} \to \Lambda\bar{\Lambda})(10^{-5})$	$\mathcal{B}(\chi_{cJ} \to \Lambda\bar{\Lambda})(\times 10^{-4})$ This work	PDG
χ_{c0}	1486 ± 42	22.80%	$3.56 \pm 0.10 \pm 0.10$	$3.64 \pm 0.10 \pm 0.10 \pm 0.07$	3.27 ± 0.24
χ_{c1}	528 ± 24	22.61%	$1.28 \pm 0.06 \pm 0.06$	$1.31 \pm 0.06 \pm 0.06 \pm 0.03$	1.14 ± 0.11
χ_{c2}	670 ± 27	20.16%	$1.82 \pm 0.08 \pm 0.17$	$1.91 \pm 0.08 \pm 0.17 \pm 0.04$	1.84 ± 0.15

uncertainties due to the uncertainties on the $\psi(3686) \to \gamma\chi_{cJ}$ branching fractions. These results, which supersede the previous BESIII measurements of branching fractions $(\chi_{cJ} \to \Lambda\bar{\Lambda})$ in Ref. [18], are consistent with the world average values [25], but not with the theoretical predictions [35–37]. This should be understood.

ACKNOWLEDGMENTS

The BESIII collaboration thanks the staff of BEPCII and the IHEP computing center for their strong support. This work is supported in part by National Key Research and Development Program of China under Contracts No. 2020YFA0406300, No. 2020YFA0406400; National Natural Science Foundation of China (NSFC) under Contracts No. 11875115, No. 11625523, No. 11635010, No. 11735014, No. 11822506, No. 11835012, No. 11935015, No. 11935016, No. 11935018, No. 11961141012; the Chinese Academy of Sciences (CAS) Large-Scale Scientific Facility Program; Joint Large-Scale Scientific Facility Funds of the NSFC and CAS under Contracts No. U1732263, No. U1832207, No. U2032110; CAS Key Research Program of Frontier Sciences under Contracts No. QYZDJ-SSW-SLH003, No. QYZDJ-SSW-SLH040; 100 Talents Program of CAS; Institute of Nuclear and Particle Physics (INPAC) and Shanghai Key Laboratory for Particle Physics and Cosmology; ERC under Contract No. 758462; European Union Horizon 2020 research and innovation programme under Contract No. Marie Sklodowska-Curie grant agreement No. 894790; German Research Foundation DFG under Contracts No. 443159800, Collaborative Research Center CRC 1044, FOR 2359, FOR 2359, GRK 214; Istituto Nazionale di Fisica Nucleare, Italy; Ministry of Development of Turkey under Contract No. DPT2006K-120470; National Science and Technology fund; Olle Engkvist Foundation under Contract No. 200-0605; STFC (United Kingdom); The Knut and Alice Wallenberg Foundation (Sweden) under Contract No. 2016.0157; The Royal Society, UK under Contracts No. DH140054, No. DH160214; The Swedish Research Council; U.S. Department of Energy under Contracts No. DE-FG02-05ER41374, No. DE-SC-0012069.

[1] D. M. Asner *et al.*, Int. J. Mod. Phys. A **24**, 499 (2009).
[2] M. Ablikim *et al.* (BESIII Collaboration), Nat. Phys. **15**, 631 (2019).
[3] T. K. Pedlar *et al.* (CLEO Collaboration), Phys. Rev. D **72**, 051108 (2005).
[4] M. Ablikim *et al.* (BESIII Collaboration), Phys. Lett. B **648**, 149 (2007).
[5] M. Ablikim *et al.* (BESIII Collaboration), Phys. Lett. B **632**, 181 (2006).
[6] M. Ablikim *et al.* (BESIII Collaboration), Phys. Rev. D **78**, 092005 (2008).
[7] M. Ablikim *et al.* (BESIII Collaboration), Phys. Rev. D **86**, 032014 (2012).
[8] M. Ablikim *et al.* (BESIII Collaboration), Phys. Rev. D **86**, 032008 (2012).
[9] M. Ablikim *et al.* (BESIII Collaboration), Phys. Rev. D **93**, 072003 (2016).
[10] M. Ablikim *et al.* (BESIII Collaboration), Phys. Rev. D **98**, 032006 (2018).
[11] M. Ablikim *et al.* (BESIII Collaboration), Phys. Rev. D **100**, 051101 (2019).
[12] M. Ablikim *et al.* (BESIII Collaboration), Phys. Rev. D **101**, 012004 (2020).
[13] M. Ablikim *et al.* (BESIII Collaboration), Phys. Rev. Lett. **125**, 052004 (2020).
[14] M. Ablikim *et al.* (BESIII Collaboration), Phys. Rev. Lett. **126**, 092002 (2021).
[15] K. Zhu, X. H. Mo, C. Z. Yuan, and P. Wang, Int. J. Mod. Phys. A **30**, 1550148 (2015).
[16] S. Dobbs, K. K. Seth, A. Tomaradze, T. Xiao, and G. Bonvicini, Phys. Rev. D **96**, 092004 (2017).
[17] R. B. Ferroli, A. Mangoni, and S. Pacetti, Eur. Phys. J. C **80**, 903 (2020).
[18] M. Ablikim *et al.* (BESIII Collaboration), Phys. Rev. D **87**, 032007 (2013).
[19] M. Ablikim *et al.* (BESIII Collaboration), Nucl. Instrum. Methods Phys. Res., Sect. A **614**, 345 (2010).
[20] C. H. Yu *et al.*, *Proceedings of IPAC2016, Busan, Korea* (2016), https://accelconf.web.cern.ch/ipac2016/.
[21] M. Ablikim *et al.* (BESIII Collaboration), Chin. Phys. C **44**, 040001 (2020).
[22] S. Agostinelli *et al.* (Geant4 Collaboration), Nucl. Instrum. Methods Phys. Res., Sect. A **506**, 250 (2003).
[23] S. Jadach, B. F. L. Ward, and Z. Was, Phys. Rev. D **63**, 113009 (2001); Comput. Phys. Commun. **130**, 260 (2000).
[24] D. J. Lange, Nucl. Instrum. Methods Phys. Res., Sect. A **462**, 152 (2001); R. G. Ping, Chin. Phys. C **32**, 599 (2008).
[25] P. A. Zyla *et al.* (Particle Data Group), Prog. Theor. Exp. Phys. **2020**, 083C01 (2020).
[26] J. C. Chen, G. S. Huang, X. R. Qi, D. H. Zhang, and Y. S. Zhu, Phys. Rev. D **62**, 034003 (2000); R. L. Yang, R. G. Ping, and H. Chen, Chin. Phys. Lett. **31**, 061301 (2014).
[27] E. Richter-Was, Phys. Lett. B **303**, 163 (1993).
[28] G. R. Liao, R. G. Ping, and Y. X. Yang, Chin. Phys. Lett. **26**, 051101 (2009).
[29] M. Xu *et al.*, Chin. Phys. C **33**, 428 (2009).
[30] M. Ablikim *et al.* (BESIII Collaboration), Chin. Phys. C **42**, 023001 (2018).

[31] M. Ablikim *et al.* (BESIII Collaboration), Phys. Rev. D **83**, 112005 (2011).
[32] M. Ablikim *et al.* (BESIII Collaboration), Phys. Rev. D **95**, 052003 (2017).
[33] M. Ablikim *et al.* (BESIII Collaboration), Phys. Rev. D **87**, 012002 (2013).
[34] P. Kessler, Nucl. Phys. **B15**, 253 (1970).
[35] R. G. Ping, B. S. Zou, and H. C. Chiang, Eur. Phys. J. A **23**, 129 (2005).
[36] X. H. Liu and Q. Zhao, J. Phys. G **38**, 035007 (2011).
[37] S. M. Wong, Eur. Phys. J. C **14**, 643 (2000).